Inorganic Chemistry
Article

Inorg. Chem. **2009**, *48*, 10789–10799 **10789**
DOI: 10.1021/ic901683c

Intermetallic Communication in Titanium(IV) Ferrocenyldiketonates

Lea T. Dulatas, Seth N. Brown,* Edema Ojomo, Bruce C. Noll, Matthew J. Cavo, Paul B. Holt, and Matthew M. Wopperer

Department of Chemistry and Biochemistry, 251 Nieuwland Science Hall, University of Notre Dame, Notre Dame, Indiana 46556-5670

Received August 25, 2009

A tetradentate bis(ferrocenyldiketonate) ligand, Fc_2BobH_2, is prepared via Claisen condensation of acetylferrocene and 2,2′-biphenyldiacetyl chloride, and is metalated with titanium(IV) isopropoxide to give $(Fc_2Bob)Ti(O^iPr)_2$ in good yield. The isopropoxide groups are replaced with di(4-nitrophenyl)phosphate groups on treatment with the corresponding acid, and with chlorides on treatment with trimethylsilyl chloride. Metathesis with catechol leads to the bis(*o*-hydroxyphenoxide) complex rather than the chelating catecholate complex. Hydrolysis selectively gives the μ-oxo trimer (Δ,Δ,Δ)/$(\Lambda,\Lambda,\Lambda)$-$\{(Fc_2Bob)Ti(\mu\text{-}O)\}_3$. The solid-state structures of the μ-oxo trimer and the bis(*o*-hydroxyphenoxide) complex show that the ferrocene substituents are oriented proximal to the biphenyl backbone rather than pointed out toward the exogenous groups. The complexes show dramatic changes in color depending on the bound anions, ranging from the red isopropoxide (λ_{max} = 489 nm) to the green bis(di(4-nitrophenyl)phosphate) (λ_{max} = 653 nm). The oxidation potentials of the ferrocenes show modest shifts based on the titanium environment, but the redox potentials of the two ferrocenes are never separated by more than 60 mV. These results and those of density-functional theory (DFT) calculations indicate that the titanium interacts principally with the lowest unoccupied molecular orbital (LUMO) of the ferrocenyldiketonate and very little with its highest occupied molecular orbital (HOMO).

Introduction

The degree to which metal centers communicate with each other electronically, as in mixed valence complexes, has attracted intense theoretical and experimental interest.[1] The nature of such electronic communication has led to insights on electron transfer processes, such as long-range electron-transfer processes in biological systems.[2] Furthermore, how intramolecular electron transfer is mediated by the intervening groups has practical implications in photochemical energy transduction and storage[3] and in molecular electronic devices.[4]

Because of its exemplary redox properties[5] and ease of synthetic modification, ferrocene has been widely used to explore the effects of intervening structures on the properties of mixed-valence compounds.[6,7] More direct through-space interactions between iron and other metals in complexes with ferrocenyl ligands have also been investigated.[8] We recently reported that the *cis*-bis(diketonate) ligand environment

*To whom correspondence should be addressed. E-mail: seth.n.brown.114@nd.edu.

(1) (a) Glover, S. D.; Goeltz, J. C.; Lear, B. J.; Kubiak, C. P. *Eur. J. Inorg. Chem.* **2009**, 585–594. (b) D'Alessandro, D. M.; Keene, F. R. *Chem. Soc. Rev.* **2006**, *35*, 424–440. (c) Demadis, K. D.; Hartshorn, C. M.; Meyer, T. J. *Chem. Rev.* **2001**, *101*, 2655–2685. (d) Launay, J. P. *Chem. Soc. Rev.* **2001**, *30*, 386–397. (e) Barbara, P. F.; Meyer, T. J.; Ratner, M. A. *J. Phys. Chem.* **1996**, *100*, 13148–13168. (f) Richardson, D. E.; Taube, H. *Coord. Chem. Rev.* **1984**, *60*, 107–128. (g) Creutz, C. *Prog. Inorg. Chem.* **1983**, *30*, 1–73.

(2) (a) Gray, H. B.; Winkler, J. R. *Proc. Nat. Acad. Sci.* **2005**, *102*, 3534–3539. (b) Blondin, G.; Girerd, J. J. *Chem. Rev.* **1990**, *90*, 1359–1376.

(3) (a) Raymo, F. M.; Tomasulo, M. *Chem. Soc. Rev.* **2005**, *34*, 327–336. (b) Schuster, D. I.; Li, K.; Guldi, D. M.; Palkar, A.; Echegoyen, L.; Stanisky, C.; Cross, R. J.; Niemi, M.; Tkachenko, N. V.; Lemmetyinen, H. *J. Am. Chem. Soc.* **2007**, *129*, 15973–15982.

(4) (a) Low, P. J. *Dalton Trans.* **2005**, 2821–2824. (b) Lent, C. S.; Isaksen, B.; Lieberman, M. *J. Am. Chem. Soc.* **2003**, *125*, 1056–1063.

(5) Geiger, W. E. *Organometallics* **2007**, *26*, 5738–5765.

(6) (a) Barlow, S.; O'Hare, D. *Chem. Rev.* **1997**, *97*, 637–669. (b) Astruc, D. *Acc. Chem. Res.* **1997**, *30*, 383–391. (c) Bildstein, B. *Coord. Chem. Rev.* **2000**, *206*, 369–394. (d) Xi, B.; Ren, T. *C. R. Chimie* **2009**, *12*, 321–331.

(7) (a) Kaufmann, L.; Breunig, J.-M.; Vitze, H.; Schödel, F.; Nowik, I.; Pichlmaier, M.; Bolte, M.; Lerner, H.-W.; Winter, R. F.; Herber, R. H.; Wagner, M. *Dalton Trans.* **2009**, 2940–2950. (b) Díez, Á.; Lalinde, E.; Moreno, M. T.; Sánchez, S. *Dalton Trans.* **2009**, 3434–3446. (c) Venkatasubbaiah, K.; Doshi, A.; Nowik, I.; Herber, R. H.; Rheingold, A. L.; Jäkle, F. *Chem.—Eur. J.* **2008**, *14*, 444–458. (d) Koridze, A. A.; Sheloumov, A. M.; Dolgushin, F. M.; Ezernitskaya, M. G.; Rosenberg, E.; Sharmin, A.; Ravera, M. *Organometallics* **2008**, *27*, 6163–6169. (e) Lim, Y.-K.; Wallace, S.; Bollinger, J. C.; Chen, X.; Lee, D. *Inorg. Chem.* **2007**, *46*, 1694–1703. (f) Figueira-Duarte, T. M.; Lloveras, V.; Vidal-Gancedo, J.; Gégout, A.; Delavaux-Nicot, B.; Welter, R.; Veciana, J.; Rovira, C.; Nierengarten, J.-F. *Chem. Commun.* **2007**, 4345–4347. (g) Mereacre, V.; Nakano, M.; Gómez-Segura, J.; Imaz, I.; Sporer, C.; Wurst, K.; Veciana, J.; Turta, C.; Ruiz-Molina, D.; Jaitner, P. *Inorg. Chem.* **2006**, *45*, 10443–10445. (h) Berry, J. F.; Cotton, F. A.; Murillo, C. A. *Organometallics* **2004**, *23*, 2503–2506. (i) Ma, K.; Fabrizi de Biani, F.; Bolte, M.; Zanello, P.; Wagner, M. *Organometallics* **2002**, *21*, 3979–3989. (j) Yip, J. H. K.; Wu, J.; Wong, K.-Y.; Yeung, K.-W.; Vittal, J. J. *Organometallics* **2002**, *21*, 1612–1621. (k) Oyaizu, K.; Yamamoto, K.; Ishii, Y.; Tsuchida, E. *Chem.—Eur. J.* **1999**, *5*, 3193–3201.

(8) (a) Shafir, A.; Arnold, J. *J. Am. Chem. Soc.* **2001**, *123*, 9212–9213. (b) Monreal, M. J.; Carver, C. T.; Diaconescu, P. L. *Inorg. Chem.* **2007**, *46*, 7226–7228.

Published on Web 10/21/2009

communicates efficiently with ligated titanium(IV) centers, causing significant asymmetric induction in binaphtholate binding through a predominantly electronic, rather than steric, influence.[9] We wondered whether this efficient electronic communication would extend beyond Lewis acid−base interactions to redox reactivity, and the development of chemically robust, geometrically well-defined bis(diketonate) ligands linked by a 2,2′-bis(methylene)biphenyl moiety ("Bob" ligands)[10,11] offered the opportunity to install two ferrocene groups in well-defined locations and to probe their interactions with each other and with the intervening titanium center. Here we describe the synthesis, structure, spectroscopy, and reactivity of such redox-active bis(diketonate)titanium(IV) complexes.

Experimental Section

Unless otherwise noted, all procedures were carried out in the drybox or on the vacuum line. Chloroform and methylene chloride were dried over 4 Å molecular sieves, followed by CaH_2. Benzene and toluene were dried over sodium, and ether and tetrahydrofuran (THF) over sodium benzophenone ketyl. Deuterated solvents were obtained from Cambridge Isotope Laboratories, dried using the same procedures as their protio analogues, and were stored in the drybox prior to use. 2,2′-Biphenyldiacetyl chloride was prepared as previously described.[10] All other reagents were commercially available and used without further purification. Routine NMR spectra were measured on a Varian VXR-300 spectrometer. Chemical shifts for ^1H and $^{13}C\{^1H\}$ spectra are reported in parts per million relative to TMS, using the known chemical shifts of the solvent residuals; those for ^{31}P are reported in parts per million referenced to external 85% H_3PO_4. Infrared spectra were recorded on KBr plates on a Perkin-Elmer PARAGON 1000 FT-IR spectrometer. Mass spectra were obtained on a JEOL LMS-AX505HA mass spectrometer using the FAB ionization mode and 3-nitrobenzyl alcohol or nitrophenyl octyl ether as a matrix. Peaks reported are the mass number of the most intense peak of isotope envelopes. UV−visible spectra were measured on dichloromethane solutions (unless otherwise noted) in 1 cm quartz cuvettes using a Beckman DU-7500 diode array spectrophotometer. Elemental analyses were performed by M-H-W Laboratories (Phoenix, AZ).

2,2′-Bis(4-ferrocenyl-2,4-dioxobutyl)biphenyl (Fc_2BobH_2, $(C_6H_4CH_2COCH_2COC_5H_4FeC_5H_5)_2$). In the drybox, 0.5524 g of 2,2′-biphenyldiacetyl chloride (1.798 mmol), 1.6489 g of acetylferrocene (7.23 mmol, 4.0 equiv), and 1.1995 g of lithium bis(trimethylsilyl)amide (7.168 mol, 4.0 equiv) were weighed into separate flasks. Dry THF (20 mL) was added to dissolve the $LiN(SiMe_3)_2$. This solution was added, with stirring, to the solid acetylferrocene to form a solution of the lithium enolate. The 2,2′-biphenyldiacetyl chloride was dissolved in THF and added dropwise with stirring to the acetylferrocene enolate solution. The reaction mixture was stirred overnight, and a precipitate formed. The reaction flask was removed from the drybox and suction filtered, and the light orange precipitate was washed with ether. The filtrate was reduced to half its volume, chilled in an ice bath for 10 min, and suction filtered to give a second crop of solid. The two batches of precipitate were combined in a 125 mL Erlenmeyer flask and stirred with a mixture of 50 mL of 0.2 M HCl and 50 mL of ether for 10 min before transferring into a separatory funnel. The top organic layer, which was dark maroon, was separated from the bottom layer, which was only slightly tinted, and set aside. The aqueous layer was extracted with a second portion of ether, and the combined organic layers were dried over $MgSO_4$ and filtered into a 250 mL round-bottom flask. This solution was evaporated to dryness, leaving a web-like foam (0.5637 g, 45%). ^1H NMR (C_6D_6): δ 16.65 (br s, 2H, enolic O*H*), 7.24 (m, 8H, aromatic protons), 5.49 (s, 2H, COC*H*CO), 4.65 (sl br s, 2H, C_5H_4 H-2), 4.62 (sl br s, 2H, C_5H_4 H-5), 4.08 (sl br s, 4H, C_5H_4 H-3,4), 3.93 (s, 10H, C_5H_5), 3.46 (s, 4H, C*HH*′). $^{13}C\{^1H\}$ NMR ($(CD_3)_2CO$; peaks due to both keto and enol forms are reported): δ 206.51, 206.23 (carbonyl), 142.01, 135.23, 132.07, 131.32, 131.04, 130.87, 128.81, 128.59, 127.71 (aromatic), 98.01 (COC*H*CO), 71.09 (C_5H_5), 73.51, 73.03, 72.86, 70.74, 70.59, 70.48, 70.32, 69.51, 69.46 (C_5H_4), 55.05, 48.61, 42.27. IR (evapd film): 3097 (m), 3059 (m), 3022 (w), 2920 (w), 1723 (s), 1659 (s), 1593 (s), 1478 (s), 1453 (s), 1412 (s), 1376 (s), 1275 (s), 1212 (m), 1187 (m), 1159 (m), 1107 (s), 1054 (m), 1030 (m), 1002 (m), 945 (m), 823 (s), 786 (m), 758 (s), 736 (s), 702 (w). UV−vis: 314 nm (23000 M^{-1} cm^{-1}), 477 nm (2800 M^{-1} cm^{-1}). FAB-MS: 690 $(M+H^+)$. Anal. Calcd for $C_{40}H_{34}Fe_2O_4$: C, 69.59%; H, 4.96%. Found: C, 69.57%; H, 4.93%.

(Fc_2Bob)Ti(O^iPr)$_2$. In the drybox, 0.3916 g of Fc_2BobH_2 (5.672×10^{-4} mol) was weighed out, dissolved in about 5 mL of benzene, and transferred into a glass bomb. To this deep red solution was added 0.7311 g of Ti(O^iPr)$_4$ (0.002572 mol, 4.5 equiv). The bomb was sealed with a Teflon valve, taken out of the drybox, and stirred overnight in a 75 °C oil bath. The reaction vessel was removed from the oil bath, attached to a vacuum line, and into it was distilled enough heptane to triple the original volume. The volume of the solution was reduced in vacuo to about 10 mL, and the product began to precipitate. The glass bomb was then taken back into the drybox where the red powdery product was collected via filtration and washed with pentane. The dark red-orange filtrate was saved in a glass vial and left overnight; a second crop of product precipitated out of solution and was collected by filtration before a third crop was collected from the filtrate following the same procedure as the first. The combined crops of (Fc_2Bob)Ti(O^iPr)$_2$ weighed 0.3271 g (64%). ^1H NMR (C_6D_6): δ 7.03 (m, 8H, aromatic protons), 5.22 (sept, 6 Hz, 2H, OC*H*(CH_3)$_2$), 4.98 (s, 2H, COC*H*CO), 4.73 (t, 1.2 Hz, 1H, C_5H_4 H-3), 4.70 (t, 1.2 Hz, 1H, C_5H_4 H-4), 4.22 (s, 10H, C_5H_5), 4.17 (m, 2H, C_5H_4 H-2 and H-5), 3.71 (d, 14 Hz, 2H, C*H*H′), 2.97 (d, 14 Hz, 2H, CH*H*′), 1.53 (d, 6 Hz, 6H, OCH(CH_3)(CH′$_3$)), 1.47 (d, 6 Hz, 6H, OCH(CH_3)(*CH*′$_3$)). $^{13}C\{^1H\}$ NMR (C_6D_6): δ 187.47, 185.98 (*C*O), 141.06, 137.12, 133.58, 129.69, 128.53, 126.55 (aromatic), 101.20 (CO*C*HCO), 80.25 (O*C*HMe$_2$), 70.50 (C_5H_5), 71.31, 71.23, 70.67, 69.90, 68.85 (C_5H_4), 46.28 (*C*H$_2$), 25.85 (OCH(*C*H$_3$)$_2$, accidentally degenerate). IR (evapd film): 3098 (w), 2966 (w), 2927 (w), 2860 (w), 1584 (m), 1553 (m), 1513 (s), 1451 (w), 1402 (m), 1376 (m), 1357 (w), 1330 (w), 1296 (m), 1214 (w), 1155 (m), 1128 (m), 1053 (w), 979 (m), 849 (w), 819 (w), 779 (w), 754 (w), 722 (w). UV−vis: 371 nm (18700 M^{-1} cm^{-1}), 492 nm (4650 M^{-1} cm^{-1}). FAB-MS: 854 $(M+H)^+$. Anal. Calcd for $C_{46}H_{46}Fe_2O_6Ti$: C, 64.66%; H, 5.43%. Found: C, 64.45%; H, 5.43%.

(Fc_2Bob)TiCl_2. In the drybox 0.0816 g (9.55×10^{-5} mol) (Fc_2Bob)Ti(O^iPr)$_2$ was weighed into a glass vial and dissolved in 4 mL of benzene. Chlorotrimethylsilane (0.2130 g, 1.961×10^{-3} mol, 20 equiv) was added, and the vial was closed with a screw cap and taken out of the drybox. The reaction mixture was then heated in a 75 °C oil bath for 22 h; dark emerald green precipitate formed on the sides of the vial, along with a lighter green film. The vial was taken back into the drybox where the dark green supernatant was pipetted off. The dark green crystalline product was washed with benzene and subsequently pentane, then dried to yield 0.0602 g of (Fc_2Bob)TiCl_2 (78%). ^1H NMR (CD_2Cl_2): δ 7.44 (t, 7 Hz, 2H, biphenyl H-4 or H-5), 7.28 (m, 6H, aromatic), 5.19 (s, 2H, CO*C*HCO), 4.75 (br m, 4H,

(9) Brown, S. N.; Chu, E. T.; Hull, M. W.; Noll, B. C. *J. Am. Chem. Soc.* **2005**, *127*, 16010–16011.
(10) Ugrinova, V.; Noll, B. C.; Brown, S. N. *Inorg. Chem.* **2006**, *45*, 10309–10320.
(11) Kongprakaiwoot, N.; Noll, B. C.; Brown, S. N. *Inorg. Chem.* **2008**, *47*, 11902–11909.

C_5H_4 H-2 and H-5), 4.71 (br m, 4H, C_5H_4 H-3 and H-4), 4.35 (s, 10H, C_5H_5), 4.00 (d, 14 Hz, 2H, C*H*H′), 3.24 (d, 14 Hz, 2H, CH*H*′). $^{13}C\{^1H\}$ NMR (CD_2Cl_2): δ 188.82, 186.45 (*C*O), 140.82, 135.79, 133.49, 130.00, 128.70, 127.75 (aromatic), 106.81 (CO*C*HCO), 75.37 (Fc *ipso*), 74.62, 74.31, 71.58 (C_5H_5), 70.99, 69.75, 45.26 (CH_2). IR (nujol mull): 2923 (s), 2724 (w), 1459 (s), 1377 (s), 1295 (w), 1213 (w), 1152 (w), 1123 (w), 1104 (w), 1028 (w), 1002 (w), 973 (w), 844 (w), 822 (w) 787 (w), 757 (w), 721 (w), 681 (w). UV−vis: 325 nm (16100 M^{-1} cm^{-1}), 639 nm (3370 M^{-1} cm^{-1}). Anal. Calcd for $C_{42}H_{32}Cl_2Fe_2O_4Ti$: C, 62.49%; H, 4.00%. Found: C, 60.18%; H, 4.76%.

(Fc$_2$Bob)Ti(OC$_6$H$_4$-2-OH)$_2$. Inside the drybox, 0.0826 g of (Fc$_2$Bob)Ti(O^{i}Pr)$_2$ (9.67×10^{-5} mol) was weighed into a 20 mL glass vial. To this was added 0.0266 g of catechol (2.42×10^{-4} mol, 2.5 equiv). The mixture was dissolved in about 4 mL of benzene, and an immediate color change in the solution was observed from red-orange to dark blood red. Pentane (~4 mL) was added to the solution by vapor diffusion over 9 h, at which point the red filtrate was decanted and the deep red-brown needles formed in the vial were washed with pentane. After drying in vacuo overnight, 0.0696 g of (Fc$_2$Bob)Ti(OC$_6$H$_4$-2-OH)$_2$ (75%) was isolated. ^{1}H NMR (C_6D_6): δ 7.71 (s, 2H, O*H*), 7.37 (dd, 7 Hz, 2 Hz, 2H, catechol H-6), 7.25 (dd, 7 Hz, 2 Hz, 2H, catechol H-3), 7.00 (m, 6H, biphenyl), 6.92 (m, 2H, biphenyl), 6.81 (m, 4H, catechol H-4,5), 4.99 (s, 2H, COC*H*CO), 4.56 (sl br, 2H, C_5H_4 H-2), 4.53 (sl br, 2H, C_5H_4 H-5), 4.14 (m, 4H, C_5H_4 H-3 and H-4), 4.05 (s, 10H, C_5H_5), 3.59 (d, 14 Hz, 2H, C*H*H′), 2.93 (d, 14 Hz, 2H, CH*H*′). $^{13}C\{^1H\}$ NMR (CD_2Cl_2): δ 190.06, 187.05 (*C*O), 156.91, 149.04, 141.09, 136.64, 134.00, 130.02, 128.92, 127.30, 123.28, 120.20, 119.36, 116.43 (aromatic), 103.73 (CO*C*HCO), 77.58 (Fc *ipso*), 73.40, 71.55, 71.42 (C_5H_5), 70.56, 70.11, 45.80 (CH_2). IR (evapd film): 3399 (w, ν_{OH}), 3082 (w), 3034 (w), 1583 (w), 1514 (s), 1489 (s), 1453 (w), 1415 (w), 1396 (w), 1366 (m), 1294 (m), 1271 (m), 1227 (w) 1203 (w), 1155 (w), 1129 (w), 1109 (w), 1059 (w), 1028 (w), 1001 (w), 978 (w), 894 (w), 819 (w), 797 (w), 745 (w), 679 (w). UV−vis: 297 nm (sh, 24000 M^{-1} cm^{-1}), 351 nm (20000 M^{-1} cm^{-1}), 534 nm (8400 M^{-1} cm^{-1}). Anal. Calcd for $C_{52}H_{42}Fe_2O_8Ti$: C, 65.43%; H, 4.44%. Found: C 65.16%; H, 4.46%.

(Fc$_2$Bob)Ti[O$_2$P(OC$_6$H$_4$NO$_2$)$_2$]$_2$. Inside the drybox, 0.0774 g of (Fc$_2$Bob)Ti(O^{i}Pr)$_2$ (9.06×10^{-5} mol) and 0.0615 g of bis(4-nitrophenyl)phosphate (Aldrich, 1.81×10^{-4} mol, 2 equiv) were weighed into a 25 mL round-bottom flask. A stirbar was added, and the flask was sealed with a needle valve, taken out of the drybox, and attached to the vacuum line. About 7 mL of CH_2Cl_2 was vacuum transferred into the flask and, with stirring, warmed to room temperature, at which point the reaction mixture began turning from dark red to purple. After about 20 min, the reaction mixture had turned dark green. It was allowed to stir at room temperature for 6 h. The solvent was removed, and another 7 mL of fresh CH_2Cl_2 was distilled into the reaction flask. After stirring overnight, the solvent was reduced to a volume of about 3 mL. The solution was then cooled to −78 °C, and two volumes of heptane were added to the stirred solution by vacuum transfer. The volume was again reduced to about 4 mL, effectively removing most of the CH_2Cl_2, before the flask was taken back into the drybox where the dark emerald green precipitate was filtered away from the brownish filtrate. The precipitate was washed with pentane and dried to yield 0.1062 g of (Fc$_2$Bob)Ti[O$_2$P(OC$_6$H$_4$NO$_2$)$_2$]$_2$ (81%). ^{1}H NMR ($CDCl_3$): δ 8.12 (d, 9 Hz, 8H, OC$_6$H$_4$NO$_2$ 3,5-H), 7.48 (d, 8 Hz, 2H, biphenyl H-6), 7.43 (d, 9 Hz, 8H, OC$_6$H$_4$NO$_2$ 2,6-H), 7.31 (m, 4H, biphenyl H-4,5), 7.10 (d, 8 Hz, 2H, biphenyl H-3), 5.17 (s, 2H, COC*H*CO), 4.76 (sl br, 2H, C_5H_4 H-2), 4.68 (sl br, 2H, C_5H_4 H-5), 4.57 (sl br, 4H, C_5H_4 H-3,4), 4.18 (s, 10H, C_5H_5), 3.98 (d, 14 Hz, 2H, C*H*H′), 3.04 (d, 14 Hz, 2H, CH*H*′). $^{13}C\{^1H\}$ NMR ($CDCl_3$): δ 191.35, 184.32 (*C*O), 156.45, 144.47, 140.46, 134.97, 133.35, 129.98, 128.80, 127.84, 125.77 (OC$_6$H$_4$NO$_2$ 3,5-C), 121.04 (sl br due to unresolved J_{PC}, OC$_6$H$_4$NO$_2$ 2,6-C), 106.79 (CO*C*HCO), 75.78, 75.40, 74.07 (Fc *ipso*), 71.88 (C_5H_5), 70.81, 70.62, 70.04, 44.70 (CH_2). $^{31}P\{^1H\}$ NMR ($CDCl_3$): δ −21.06. IR (nujol mull): 2726 (w), 2678 (w), 1613 (w), 1590 (w), 1518 (s), 1345 (s), 1297 (m), 1271 (m), 1214 (m), 1161 (w), 1109 (w), 1066 (w), 1007 (w), 974 (w), 918 (m), 854 (w), 818 (w), 750 (w), 722 (w). UV−vis: 276 nm (54800 M^{-1} cm^{-1}), 661 nm (5360 M^{-1} cm^{-1}). Anal. Calcd for $C_{67}H_{55}Fe_2N_4O_{20}P_2Ti$: C, 55.20%; H, 3.80%. Found: C 55.30%; H, 4.05%.

(Fc$_2$Bob)Ti(O^{i}Pr)[O$_2$P(OC$_6$H$_4$NO$_2$)$_2$]. In the drybox, 0.0808 g of (Fc$_2$Bob)Ti(O^{i}Pr)$_2$ (9.46×10^{-5} mol) and 0.0352 g of bis(4-nitrophenyl) phosphate (1.04×10^{-4} mol, 1.1 equiv) were weighed into a 20 mL glass vial and dissolved in about 4 mL of benzene. The color changed from red-orange to reddish purple immediately. Pentane (~4 mL) was added by vapor diffusion overnight. The dark red-purple filtrate was pipetted off, leaving a reddish purple precipitate and some purple-colored film in the bottom of the vial. The solids were slurried with about 3 mL of hexanes, filtered, and dried to give 0.0872 g (81%) of the monoalkoxide product. ^{1}H NMR ($CDCl_3$): δ 8.04 (d, 9 Hz, 2H, POAr 3,5-H), 8.02 (d, 9 Hz, 2H, POAr′ 3,5-H), 7.42 (m, 2H, biphenyl), 7.38 (d, 9 Hz, 2H, POAr 2,6-H), 7.34 (d, 9 Hz, 2H, POAr′ 2,6-H), 7.28 (m, 3H, biphenyl), 7.21 (m, 2H, biphenyl), 7.00 (d, 8 Hz, 1H, biphenyl), 5.02 (s, 1H, COC*H*CO), 5.01 (sept, 6 Hz, 1H, OC*H*(CH$_3$)$_2$), 5.01 (s, 1H, COC*H*CO), 4.59 (m, 1H, C_5H_4 H-2), 4.58 (sl br, 1H, C_5H_4 H-2′), 4.53 (m, 2H, C_5H_4), 4.49 (m, 2H, C_5H_4), 4.43 (sl br, 1H, C_5H_4 H-5), 4.37 (m, 1H, C_5H_4 H-5′), 4.18 (s, 5H, C_5H_5), 4.17 (s, 5H, $C_5H'_5$), 3.97 (d, 14 Hz, 1H, C*H*H′), 3.85 (d, 14 Hz, 1H, C*H*H′), 3.22 (d, 14 Hz, 1H, CH*H*′), 2.91 (d, 14 Hz, 1H, CH*H*′), 1.38 (d, 6 Hz, 3H, OCH(C*H*$_3$)(CH′$_3$)), 1.37 (d, 6 Hz, 3H, OCH(CH$_3$)(C*H*′$_3$)). $^{13}C\{^1H\}$ NMR ($CDCl_3$): δ 190.36, 188.37, 186.47, 184.87 (*C*O), 157.26, 157.21 (PO*C*), 143.88, 143.82 (*C*NO$_2$), 140.70, 140.58, 136.20, 135.53, 133.44, 133.31, 130.07, 129.62, 128.46, 128.31, 127.29, 127.19 (biphenyl), 125.55 (POAr 3,5-C), 125.53 (POAr′ 3,5-C), 120.94 (d, J_{PC} = 6 Hz, POAr 2,6-C), 120.70 (d, J_{PC} = 6 Hz, POAr′ 2,6-C), 103.99, 102.90 (CO*C*HCO), 83.90 (TiO*C*H[CH$_3$]$_2$), 76.24, 73.40, 73.02, 72.48, 72.44, 70.86 (C_5H_5), 70.62 (C'_5H_5), 70.47, 70.08, 69.81, 69.52, 68.34 (C_5H_4), 46.01, 45.27 (CH_2), 24.80, 24.78 (TiOCH[*C*H$_3$][*C*′H$_3$]). IR (nujol mull): 2724 (w), 1612 (w), 1589 (m), 1347 (s), 1288 (m), 1215 (m), 1155 (w), 1107 (w), 1053 (w), 973 (m), 916 (w), 854 (w), 748 (w), 685 (w). UV−vis: 286 nm (27500 M^{-1} cm^{-1}), 372 nm (9500 M^{-1} cm^{-1}), 540 nm (3600 M^{-1} cm^{-1}). Anal. Calcd for $C_{55}H_{47}Fe_2N_2O_{13}PTi$: C, 58.22%; H, 4.18%. Found: C, 57.24%; H, 3.96%.

{(Fc$_2$Bob)Ti(μ-O)}$_3$. (Fc$_2$Bob)Ti(O^{i}Pr)$_2$ (0.1025 g, 1.12×10^{-4} mol) was weighed out in a glass scintillation vial and dissolved in about 10 mL of THF in the air. Three drops of deionized water were added, the vial sealed, and the reaction mixture allowed to stir overnight. The rose-red precipitate was then vacuum filtered and washed with pentane to yield 0.1024 g (97%) of the μ-oxo trimer. ^{1}H NMR ($CDCl_3$): δ 7.47 (m, 12H, biphenyl), 7.32 (d, 7 Hz, 6H, biphenyl), 7.28 (m, 6H, biphenyl), 5.57 (br s, 6H, C_5H_4 H-2 or -5), 5.03 (s, 6H, COC*H*CO), 4.29 (s, 30H, C_5H_5), 4.16 (br s, 6H, C_5H_4 H-3 or -4), 4.06 (br s, 6H, C_5H_4 H-3 or -4), 3.92 (d, 14 Hz, 6H, C*H*H′), 3.90 (br s, 6H, C_5H_4 H-2 or -5), 3.06 (d, 14 Hz, 6H, CH*H*′). $^{13}C\{^1H\}$ NMR (THF-d_8): δ 188.64 (*C*O), 186.54 (*C*O), 142.65, 137.48, 134.56, 130.70, 129.06, 127.27, 103.65 (CO*C*HCO), 73.59, 71.77, 71.34 (C_5H_5), 70.93, 68.02, 47.09 (CH_2) [*ipso* C_5H_4 not found]. IR (evaporated film): 3096 (w), 3060 (w), 3016 (w), 2918 (w), 2847 (w), 1550 (s), 1510 (s), 1448 (m), 1399 (m), 1373 (s), 1333 (m), 1315 (m), 1293 (m), 1213 (w), 1151 (w), 1129 (w), 1107 (w), 1054 (w), 1027 (w), 1005 (w), 974 (w), 907 (w), 841 (w), 796 (m), 752 (m), 730 (m). Anal. Calcd for $C_{120}H_{96}Fe_6O_{15}Ti_3$: C, 63.87; H, 4.29. Found: C, 62.23; H, 4.12.

Cyclic Voltammetry. Cyclic voltammetry was performed in the drybox using an EG&G Instruments PAR 283 or a BAS

Epsilon potentiostat. A standard three-electrode setup was used, with a glassy carbon working electrode, Pt or glassy carbon counter electrode, and a silver/silver chloride pseudo-reference electrode. The electrodes were connected to the potentiostat through electrical conduits in the drybox wall. Samples were approximately 1 mM in CH_2Cl_2, using 0.1 M Bu_4NPF_6 as the electrolyte. Potentials were referenced to ferrocene/ferrocenium at 0 V,[12] with the reference potential established by spiking the test solution with a small amount of ferrocene. Cyclic voltammograms were recorded with a scan rate of 60 mV s^{-1}.

Density Functional Theory (DFT) Calculations. Geometry optimizations and orbital calculations were performed on the model compounds $(FcCOCHCH_3)_2TiCl_2$ and the free (enolized) β-diketone $FcC[OH]=CHC(O)CH_3$ using the hybrid B3LYP method, with a 6-31G* basis set for all atoms, using the Gaussian03 suite of programs.[13] This method and basis set have been shown to do a good job reproducing the geometries of other diketonate-titanium complexes.[9] The starting geometries were derived from the crystal structure of $(Fc_2Bob)Ti(OC_6H_4\text{-}2\text{-}OH)_2$, with the bis(methylene)biphenyl linker replaced by methyl groups. The titanium was replaced by a hydrogen on the ferrocenyl carbonyl for the free ligand, and the catecholate groups replaced by chloride, at an initial Ti−Cl distance of 2.28 Å, in $(FcCOCHCH_3)_2TiCl_2$. Only the *cis*-α isomer of $(FcCOCHCH_3)_2TiCl_2$ with axial ferrocenes (most relevant to $(Fc_2Bob)TiX_2$) was analyzed. The molecular symmetries were not constrained in the calculations (although the geometry of the titanium dichloride complex was extremely close to C_2). Optimized geometries were confirmed to be minima by frequency analysis. Plots of calculated Kohn−Sham orbitals (Figure 6 and Supporting Information, Figure S2) were generated using the program GaussView (v. 3.09) using a contour value of 0.03.

X-ray Crystallography of $(Fc_2Bob)Ti(OC_6H_4\text{-}2\text{-}OH)_2$ and $\{(Fc_2Bob)Ti(\mu\text{-}O)\}_3\cdot 2C_4H_8O\cdot 2CHCl_3$. Deep red blocks of $(Fc_2Bob)Ti(OC_6H_4\text{-}2\text{-}OH)_2$ were grown by vapor diffusion of pentane directly into the crude reaction mixture in benzene. The μ-oxo trimer was crystallized on the benchtop by vapor diffusion of THF into a chloroform solution of the compound. The crystals were placed in Paratone oil before transferring to MiTeGen MicroMounts to be placed in the cryogenic (T = 100 K) N_2 stream of a Bruker Apex CCD diffractometer. Data were reduced, correcting for absorption, using the SADABS program. The space groups were determined in both cases to be $P2_1/n$ based on the systematic absences. The structures were solved using direct methods, with all non-hydrogen atoms not apparent from the initial solution found on difference Fourier maps. All heavy atoms were refined anisotropically.

In the structure of the bis(catecholate) complex, one of the catecholate rings was disordered, with the benzene ring shifted slightly and with the hydroxyl group on the opposite side. The benzene ring of the minor component of the disorder was refined as a regular hexagon, with the C−O distance to the free hydroxyl group restrained to a chemically reasonable value (free refinement was unreliable because of the close approach of this atom to a carbon atom on the benzene ring of the major component). Thermal parameters of the minor component were constrained to be equivalent to the thermal parameters of the corresponding atoms in the major component, whose occupancy refined to 75.7(2)%. All hydrogen atoms were found on difference maps and refined isotropically, except for those on the disordered catechol ring, which were placed in calculated positions.

In the structure of the μ-oxo trimer, two of the ferrocenes were disordered, one near Fe11 with an alternate location of the $(C_5H_5)Fe$ fragment (refined to 30.17(15)% occupancy), and one near Fe32 where the entire $(C_5H_5)Fe(C_5H_4)$ unit was refined in two locations (the minor component refined to 39.84(8)% occupancy). Thermal parameters of the minor components were constrained to be equivalent to the thermal parameters of the corresponding atoms in the major components. Hydrogens were placed in calculated positions. Several molecules of chloroform and THF could be discerned in the lattice voids, but severe disorder precluded satisfactory refinement. The lattice solvent was treated using the SQUEEZE routine in the program PLATON,[14] which found electron density corresponding to two $CHCl_3$ and two THF molecules per trimer.

All calculations used SHELXTL (Bruker AXS),[15] with scattering factors and anomalous dispersion terms taken from the literature.[16] Further details about the individual structures are given in Table 1.

Table 1. Crystal Data for $(Fc_2Bob)Ti(OC_6H_4\text{-}2\text{-}OH)_2$ and $\{(Fc_2Bob)Ti(\mu\text{-}O)\}_3\cdot 2CHCl_3\cdot 2THF$

	$(Fc_2Bob)Ti(OC_6H_4\text{-}2\text{-}OH)_2$	$\{(Fc_2Bob)Ti(\mu\text{-}O)\}_3\cdot 2CHCl_3\cdot 2THF$
empirical formula	$C_{52}H_{42}Fe_2O_8Ti$	$C_{130}H_{114}Cl_6Fe_6O_{17}Ti_3$
temperature (K)	100(2)	100(2)
λ	0.71073 Å (Mo Kα)	0.71073 Å (Mo Kα)
space group	$P2_1/n$	$P2_1/n$
total data collected	77083	222767
no. of indep reflns.	10421	45830
R_{int}	0.0388	0.0282
obsd. refls. [$I > 2\sigma(I)$]	8671	35164
a (Å)	13.6137(4)	15.8856(9)
b (Å)	18.0630(5)	24.3763(14)
c (Å)	18.0160(5)	30.8018(17)
α (deg)	90	90
β (deg)	109.750(2)	92.654(3)
γ (deg)	90	90
V (Å^3)	4169.6(2)	11914.7(12)
Z	4	4
cryst size (mm)	0.12 × 0.20 × 0.36	0.23 × 0.40 × 0.41
no. refined params.	726	1350
R indices [$I > 2\sigma(I)$][a]	$R1$ = 0.0350, $wR2$ = 0.0864	$R1$ = 0.0418, $wR2$ = 0.1183
R indices (all data)[a]	$R1$ = 0.0462, $wR2$ = 0.0936	$R1$ = 0.0558, $wR2$ = 0.1245
goodness of fit	1.034	1.133

[a] $R1 = \sum||F_o| - |F_c||/\sum|F_o|$; $wR2 = [\sum w(F_o^2 - F_c^2)^2/\sum w(F_o^2)^2]^{1/2}$.

(12) Connelly, N. G.; Geiger, W. E. *Chem. Rev.* **1996**, *96*, 877–910.
(13) Frisch, M. J.; Trucks, G. W.; Schlegel, H. B.; Scuseria, G. E.; Robb, M. A.; Cheeseman, J. R.; Montgomery, J. A.; Vreven, T.; Kudin, K. N.; Burant, J. C.; Millam, J. M.; Iyengar, S. S.; Tomasi, J.; Barone, V.; Mennucci, B.; Cossi, M.; Scalamani, G.; Rega, N.; Petersson, G. A.; Nakatsuji, H.; Hada, M.; Ehara, M.; Toyota, K.; Fukuda, R.; Hasegawa, J.; Ishida, M.; Nakajima, T.; Honda, Y.; Kitao, O.; Nakai, H.; Klene, M.; Li, X.; Knox, J. E.; Hratchian, H. P.; Corss, J. B.; Adamo, C.; Jaramillo, J.; Gomperts, R.; Stratmann, R. E.; Yazyev, O.; Austin, A. J.; Cammi, R.; Pomelli, C.; Ochterski, J. W.; Ayala, P. Y.; Morokuma, K.; Voth, G. A.; Salvador, P.; Dannenberg, J. J.; Zakrzewski, V. G.; Dapprich, S.; Daniels, A. D.; Strain, M. C.; Farkas, O.; Malick, D. K.; Rabuck, A. D.; Raghavachari, K.; Foresman, J. B.; Ortiz, J. V.; Cui, Q.; Baboul, A. G.; Clifford, S.; Cioslowski, J.; Stefanov, B. B.; Liu, G.; Liashenko, A.; Piskorz, P.; Komaromi, I.; Martin, R. L.; Fox, D. J.; Keith, T.; Al-Laham, M. A.; Peng, C. Y.; Nanayakkara, A.; Challacombe, M.; Gill, P. M. W.; Johnson, B.; Chen, W.; Wong, M. W.; Gonzalez, C.; Pople, J. A. *Gaussian 03*, Revision C.01; Gaussian Inc.: Wallingford, CT, 2004.
(14) Spek, A. L. *J. Appl. Crystallogr.* **2003**, *36*, 7–13.
(15) Sheldrick, G. M. *Acta Crystallogr. A* **2008**, *A64*, 112–122.
(16) *International Tables for Crystallography*; Kluwer Academic Publishers: Dordrecht, The Netherlands, 1992; Vol C.

Results and Discussion

Synthesis and Characterization of 2,2′-Biphenylbis(4-ferrocenyl-2,4-butanedione) and Its Titanium Complexes. We have previously found Claisen condensation between lithium enolates of methyl ketones and mono-[17,18] and diacyl chlorides[10] to be an efficient route to a variety of β-diketonate ligands. Thus, reaction of the lithium enolate of acetylferrocene, generated in THF using lithium hexamethyldisilazide, with 2,2′-biphenyldiacetyl chloride, gives 2,2′-biphenylbis(4-ferrocenyl-2,4-butanedione) (Fc_2BobH_2) in moderate yield (eq 1). Claisen condensations between acetylferrocene and esters or acyl chlorides have been used to prepare ferrocenyldiketones,[19] but the presence of reactive α-hydrogens in biphenyldiacetyl chloride in this instance requires the use of 4 equiv of enolate (rather than allowing the use of 2 equiv of enolate and two of an inexpensive sacrificial base). As previously observed,[10] a key feature of the preparation is precipitation of the dilithium salt $Li_2(Fc_2Bob)$, which allows protonation to give the free bis(β-diketone) directly in pure form. In contrast to previous syntheses, diethyl ether is not a suitable solvent for this reaction because the lithium enolate of acetylferrocene is only sparingly soluble in ether, both depressing the conversion and leading to a product contaminated with acetylferrocene. NMR spectra of Fc_2BobH_2 in $CDCl_3$, C_6D_6, or acetone-d_6 are most consistent with the diketones being largely but not entirely enolized, with a prominent peak far downfield (e.g., δ 16.65 in C_6D_6), but with small additional peaks attributable to the keto form(s) of the compound. Keto−enol mixtures have been observed in other ferrocenyl-β-diketones.[20]

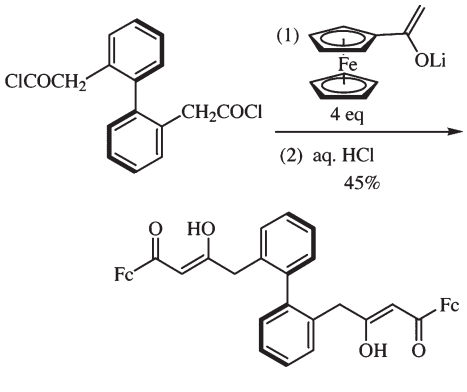

(1)

The bis(β-diketone) Fc_2BobH_2 is metalated by titanium isopropoxide on heating overnight in benzene (eq 2). As previously observed for the *p*-tolyl and *tert*-butyl derivatives, reaction takes place immediately at room temperature, but about half of the material is polymeric, and heating overnight in the presence of excess $Ti(O^iPr)_4$ is required to convert the material into the C_2-symmetric monomer.[10] Formation of $(Fc_2Bob)Ti(O^iPr)_2$ is accompanied by a dramatic separation of the two diastereotopic methylene protons in the ^1H NMR spectrum ($\Delta\delta$ = 0.74 ppm in C_6D_6), contrasting with the nearly degenerate chemical shifts observed in the free ligand. There is little change in color on metalation, with both the free ligand Fc_2BobH_2 and the titanium alkoxide complex appearing red-orange.

Table 2. Selected Bond Distances (Å) and Angles (deg) in $(Fc_2Bob)Ti(OC_6H_4\text{-}2\text{-}OH)_2$

Ti−O1	1.9894(14)	O1−Ti−O2	83.51(6)
Ti−O2	1.9732(13)	O1−Ti−O3	81.34(5)
Ti−O3	1.9892(13)	O1−Ti−O4	96.02(6)
Ti−O4	2.0142(13)	O1−Ti−O5	166.38(6)
Ti−O5	1.8597(14)	O1−Ti−O6	91.94(6)
Ti−O6	1.8213(13)	O2−Ti−O3	91.91(5)
		O2−Ti−O4	175.70(5)
		O2−Ti−O5	85.05(6)
		O2−Ti−O6	95.73(6)
		O3−Ti−O4	83.80(5)
		O3−Ti−O5	91.71(6)
		O3−Ti−O6	169.20(6)
		O4−Ti−O5	94.84(6)
		O4−Ti−O6	88.55(6)
		O5−Ti−O6	96.53(7)
		Ti−O5−C51	131.42(15)
		Ti−O6−C61	165.64(14)

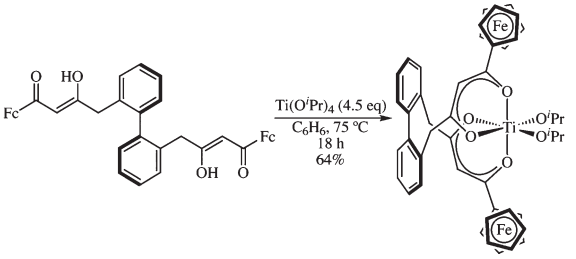

(2)

The isopropoxide groups in $(Fc_2Bob)Ti(O^iPr)_2$ are readily replaced by Brønsted or Lewis acidic reagents. Thus, treatment of the diisopropoxide with 1 equiv of di(4-nitrophenyl)phosphate, $(O_2NC_6H_4O)_2P(O)(OH)$, gives the violet monoalkoxide complex $(Fc_2Bob)Ti(O^iPr)$-$(O_2P[OC_6H_4NO_2]_2)$, while treatment with two or more equivalents of phosphate gives the green bis(phosphate) complex $(Fc_2Bob)Ti(O_2P[OC_6H_4NO_2]_2)_2$ (eq 3). The former complex shows distinct ^1H and ^{13}C NMR resonances for the diketonate arms *trans* to the alkoxide and diarylphosphate ligands, as expected given the complex's C_1 symmetry, and the two nitrophenyl groups in this monophosphate complex are diastereotopic. However, both ^1H and ^{13}C NMR spectra indicate that all four nitrophenyl groups in $(Fc_2Bob)Ti(O_2P[OC_6H_4NO_2]_2)_2$ are equivalent on the NMR time scale at room temperature. Presumably there is some process which interconverts the diastereotopic aryl groups, most likely an $O\rightarrow O'$ isomerization of the phosphates. The fact that this process is more rapid in the bis(phosphate) than in the monoalkoxide complex suggests that it takes place through a seven-coordinate intermediate,

(17) Fortner, K. C.; Bigi, J. P.; Brown, S. N. *Inorg. Chem.* **2005**, *44*, 2803–2814.

(18) Schroeder, T.; Ugrinova, V.; Noll, B. C.; Brown, S. N. *Dalton Trans.* **2006**, 1030–1040.

(19) (a) du Plessis, W. C.; Vosloo, T. G.; Swarts, J. C. *J. Chem. Soc., Dalton Trans.* **1998**, 2507–2514. (b) Abiko, A.; Wang, G. *Tetrahedron* **1998**, *54*, 11405–11420. (c) Woisetschläger, O. E.; Geisbauer, A.; Polborn, K.; Sünkel, K.; Beck, W. *Z. Anorg. Allg. Chem.* **1999**, *625*, 2164–2168.

(20) du Plessis, W. C.; Davis, W. L.; Cronje, S. J.; Swarts, J. C. *Inorg. Chim. Acta* **2001**, *314*, 97–104.

(21) The data are also consistent with the seven-coordinated structure being the stable form of the complex, with the six-coordinate structure being readily accessible. This seems less likely, as structurally characterized examples of seven-coordinate titanium bis(diketonates) are rare, though $(\eta^5\text{-}C_5H_3[SiMe_3]_2)Ti(\kappa^2\text{-}CF_3COCHCOCF_3)_2(\kappa^1\text{-}O_3SCF_3)$ has been characterized: Winter, C. H.; Zhou, X.-X.; Heeg, M. J. *Organometallics* **1991**, *10*, 3799–3801.

$(Fc_2Bob)Ti(\eta^1\text{-}O_2P[OAr]_2)(\eta^2\text{-}O_2P[OAr]_2)$. The more strongly donating alkoxide ligand would make the titanium less electrophilic and retard formation of the higher-coordinate species.[21]

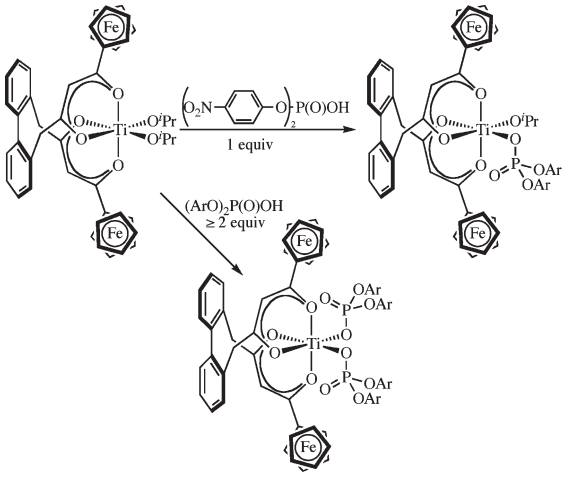

(3)

Chlorotrimethylsilane behaves analogously to di(4-nitrophenyl)phosphate. Reaction of $(Fc_2Bob)Ti(O^iPr)_2$ with excess Me_3SiCl gives the green dichloride complex $(Fc_2Bob)TiCl_2$ (eq 4). The violet monochloride complex $(Fc_2Bob)Ti(O^iPr)(Cl)$ is observed by NMR as an intermediate in this reaction, but was not isolated in pure form.

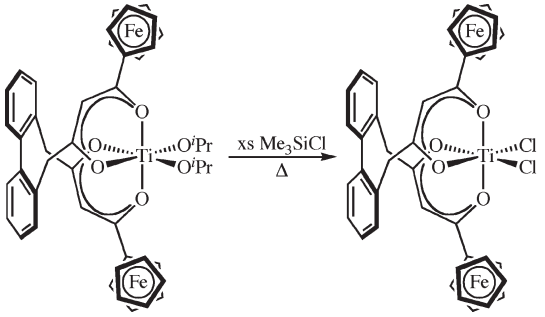

(4)

Preparation and Characterization of a Bis(monoprotonated catecholate) Complex. Catechol also replaces the isopropoxide groups in $(Fc_2Bob)Ti(O^iPr)_2$. The major product of this reaction is not, however, the expected chelated catecholate complex $(Fc_2Bob)Ti(O_2C_6H_4)$, but rather $(Fc_2Bob)Ti(OC_6H_4\text{-}2\text{-}OH)_2$, where two moles of catechol react, each retaining an intact *ortho* hydroxy group. Even when equimolar quantities of catechol and $(Fc_2Bob)Ti(O^iPr)_2$ react, the chelated catecholate complex is not observed in significant concentration; rather, the major species present are unreacted starting material and bis(aryloxide). Given the very fast reaction (color change is immediate on mixing) and the general kinetic facility of intramolecular reactions, it seems likely that the preference for the monodentate complex is thermodynamic in origin. The bis(2-hydroxyphenoxide) complex $(Fc_2Bob)Ti(OC_6H_4\text{-}2\text{-}OH)_2$ is isolated in good yield when 2 equiv of catechol are employed (eq 5). Spectroscopic and analytical data, including the observation of an O−H stretch at 3399 cm^{-1} in the IR and a 2H resonance attributable to the O*H* protons at δ 7.71 ppm (C_6D_6), strongly support the proposed structure.

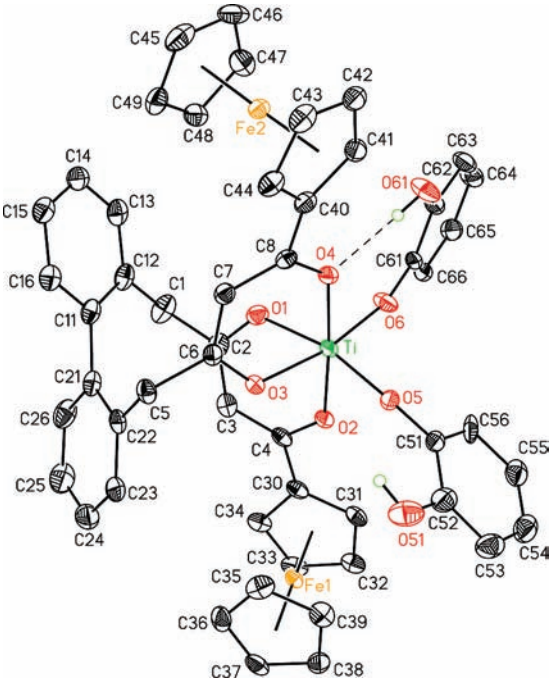

Figure 1. Thermal ellipsoid plot (50% ellipsoids) of $(Fc_2Bob)Ti(OC_6H_4\text{-}2\text{-}OH)_2$. Hydrogens (except those bonded to oxygen) are omitted for clarity, and only the major component of the disordered 2-hydroxyphenyl group (C61−C66 and O61) is shown.

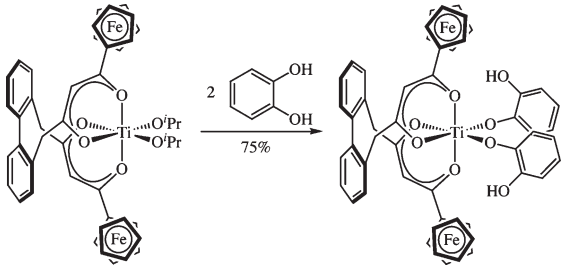

(5)

Confirmation of the proposed structure is provided by crystallographic analysis (Tables 1, 2, Figure 1). The relative configuration of the biphenyl and the titanium, the (*S*,Δ)/(*R*,Λ) diastereomer, is the same as that observed previously in bis(methylene)biphenyl-bridged bis(diketonate)[10] and hydroxamate-diketonate[11] complexes. The 2-hydroxyphenoxide ligands form short Ti−O bonds (1.84 Å avg.), only slightly longer than observed in other bis(diketonate)-diaryloxide complexes $(^tBu_2Bob)Ti(O\text{-}2,6\text{-}^iPr_2C_6H_3)_2$ (1.8173(11) Å),[10] $(acac)_2Ti(O\text{-}2,6\text{-}^iPr_2C_6H_3)_2$ (1.834(5) Å),[22] or $(TolCOCHCOC_6H_4CH_2CH_2C_6H_2\text{-}3,5\text{-}^tBu_2\text{-}2\text{-}O)_2Ti$ (1.830 Å avg.).[18] In contrast, the only other crystallographically characterized 2-hydroxyaryloxide complex, anionic $(Et_3NH)_2[Ti(DTBC)_2(HDTBC)]_2\cdot 2CHCl_3$ (DTBC = 3,5-di-*tert*-butylcatecholate), has a much longer Ti−O distance (1.936(2) Å).[23] The somewhat obtuse angle between the aryloxides (O5−Ti−O6 = 96.53(7)°) is also similar to that observed in previously characterized $(dike)_2Ti(OAr)_2$ complexes (dike = β-diketonate). At least

(22) Bird, P. H.; Fraser, A. R.; Lau, C. F. *Inorg. Chem.* **1973**, *12*, 1322–1328.
(23) Borgias, B. A.; Cooper, S. R.; Koh, Y. B.; Raymond, K. N. *Inorg. Chem.* **1984**, *23*, 1009–1016.

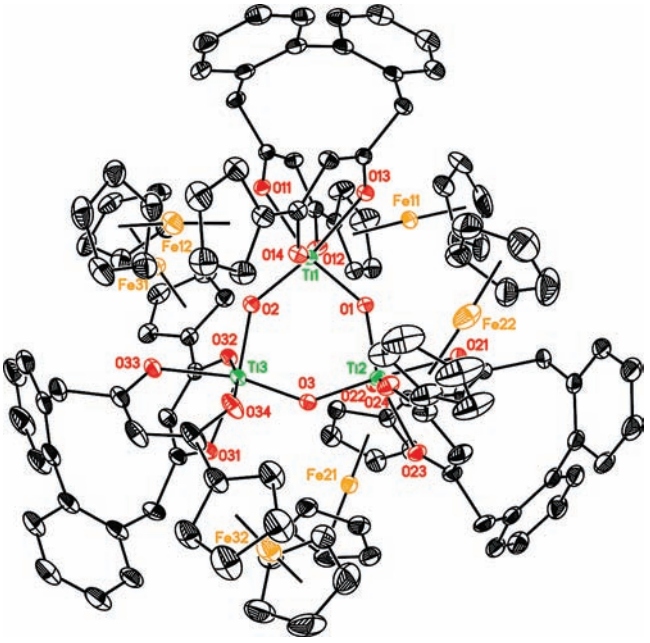

Figure 2. Thermal ellipsoid plot (50% ellipsoids) of the metal complex of $\{(Fc_2Bob)Ti(\mu\text{-}O)\}_3 \cdot 2CHCl_3 \cdot 2THF$. Hydrogen atoms and minor components of the disordered ferrocene groups are omitted for clarity.

in the solid state, one of the phenolic O−H groups forms a hydrogen bond to one of the diketonate carbonyl oxygens; this may explain the significant elongation of the Ti−O4 distance over the otherwise equivalent bond to O2 (2.0142(13) Å and 1.9732(13), respectively; note that the two chemically equivalent titanium−oxygen distances *trans* to the aryloxides are observed to be equal within experimental error). Several features of the conformation of the ferrocene groups in $(Fc_2Bob)Ti(OC_6H_4\text{-}2\text{-}OH)_2$ are of interest. The C_5H_4 rings bonded to the diketonate are essentially coplanar with the diketonate ring, as is typically observed in aryl- and ferrocenyldiketonate complexes. In both arms, the CpFe group projects inward toward the other diketonate and the bis(methylene)biphenyl bridge, rather than outward toward the aryloxide ligands (Supporting Information, Figure S1).

Table 3. Selected Bond Distances (Å) and Angles (deg) in $\{(Fc_2Bob)Ti(\mu\text{-}O)\}_3 \cdot 2CHCl_3 \cdot 2THF$

	n = 1	n = 2	n = 3
Ti*n*-O*n*1	2.0795(9)	2.1158(9)	2.0932(9)
Ti*n*-O*n*2	1.9823(10)	1.9800(10)	1.9716(9)
Ti*n*-O*n*3	2.1121(9)	2.0700(9)	2.1088(9)
Ti*n*-O*n*4	1.9835(9)	1.9852(10)	1.9720(10)
Ti*n*-O1	1.8046(9)	1.8192(9)	
Ti*n*-O2	1.8153(9)		1.8177(9)
Ti*n*-O3		1.8091(9)	1.8203(9)
O*n*1-Ti*n*-O*n*2	80.27(4)	81.14(4)	81.60(4)
O*n*1-Ti*n*-O*n*3	76.88(3)	77.64(4)	77.76(4)
O*n*1-Ti*n*-O*n*4	91.42(4)	96.42(4)	89.54(4)
O*n*2-Ti*n*-O*n*3	92.80(4)	89.04(4)	88.77(4)
O*n*2-Ti*n*-O*n*4	170.77(4)	169.79(4)	168.01(4)
O*n*3-Ti*n*-O*n*4	81.34(4)	80.76(4)	81.43(4)
O*n*1-Ti*n*-O1	160.59(4)	87.05(4)	
O*n*1-Ti*n*-O2	95.22(4)		165.79(4)
O*n*1-Ti*n*-O3		166.93(4)	91.32(4)
O*n*2-Ti*n*-O1	86.08(4)	103.60(4)	
O*n*2-Ti*n*-O2	97.73(4)		87.69(4)
O*n*2-Ti*n*-O3		86.30(4)	99.57(4)
O*n*3-Ti*n*-O1	90.18(4)	158.48(4)	
O*n*3-Ti*n*-O2	165.62(4)		92.77(4)
O*n*3-Ti*n*-O3		98.65(4)	165.22(4)
O*n*4-Ti*n*-O1	100.98(4)	86.11(4)	
O*n*4-Ti*n*-O2	86.94(4)		99.60(4)
O*n*4-Ti*n*-O3		95.32(4)	88.64(5)
O1−Ti*n*-O2	100.26(4)		
O1−Ti*n*-O3		99.47(4)	
O2−Ti*n*-O3			99.69(4)
Ti1−O*n*-Ti2	140.25(5)		
Ti1−O*n*-Ti3		139.52(5)	
Ti2−O*n*-Ti3			140.58(5)

The apparent instability of the chelated catecholate complex $(Fc_2Bob)Ti(O_2C_6H_4)$ is surprising, given the abundance of titanium(IV) catecholate complexes; in particular tris(catecholate) anions $[Ti(cat)_3]^{2-}$ are well-studied and very stable.[24,25] Since the chelated complex must be entropically favored, the bonding in the bis(monodentate) complex must be markedly stronger. We attribute this to enhanced aryloxide-to-titanium π donation in the bis(monodentate) complex. While there is probably some π donation from the diketonates to titanium in the $(dike)_2Ti^{2+}$ fragment,[26] at the relatively long Ti−O diketonate distances of 1.94−2.08 Å, this π donation is not expected to be strong. Furthermore, since each diketonate has only one good π donor orbital, only two of the three titanium dπ orbitals (one each of A and B symmetry in C_2-symmetric $(dike)_2TiX_2$) are engaged in π bonding to any extent; the third dπ orbital (of A symmetry) is strictly nonbonding.[9] The $(dike)_2Ti^{2+}$ fragment is thus expected to be a rather strong π Lewis acid. The chelated catecholate ligand is ill-suited to interact with these empty orbitals for two reasons. First, the relatively small Ti−O−C angles required by the five-membered chelate ring (typically about 115°)[23,25] mean that the oxygen lone pairs in the plane of the catecholate have a high degree of *s* character and hence

(24) (a) Davies, J. A.; Dutremez, S. G. *Inorg. Synth.* **1997**, *31*, 11–14. (b) Martin, J. L.; Takats, J. *Can. J. Chem.* **1975**, *53*, 572–577. (c) Gut, R.; Schmid, E.; Serrallach, J. *Helv. Chim. Acta* **1971**, *54*, 609–624. (d) Sever, M. J.; Wilker, J. J. *Dalton Trans.* **2004**, 1061–1072.

(25) (a) Hahn, F. E.; Rupprecht, S.; Moock, K. H. *J. Chem. Soc., Chem. Commun.* **1991**, 224–225. (b) Karpishin, T. B.; Stack, T. D. P.; Raymond, K. N. *J. Am. Chem. Soc.* **1993**, *115*, 182–192. (c) Albrecht, M.; Kotila, S. *Angew. Chem., Int. Ed.* **1995**, *34*, 2134–2137. (d) Albrecht, M.; Röttele, H.; Burger, P. *Chem.—Eur. J.* **1996**, *2*, 1264–1268. (e) Albrecht, M.; Kotila, S. *Angew. Chem., Int. Ed. Engl.* **1996**, *35*, 1208–1210. (f) Albrecht, M.; Fröhlich, R. *J. Am. Chem. Soc.* **1997**, *119*, 1656–1661. (g) Albrecht, M.; Schneider, M.; Fröhlich, R. *New J. Chem.* **1998**, *22*, 753–754. (h) Brückner, C.; Powers, R. E.; Raymond, K. N. *Angew. Chem., Int. Ed.* **1998**, *37*, 1837–1839. (i) Scherer, M.; Caulder, D. L.; Johnson, D. W.; Raymond, K. N. *Angew. Chem., Int. Ed.* **1999**, *38*, 1588–1592. (j) Sun, X.; Johnson, D. W.; Caulder, D. L.; Powers, R. E.; Raymond, K. N.; Wong, E. H. *Angew. Chem., Int. Ed.* **1999**, *38*, 1303–1307. (k) Caulder, D. L.; Brückner, C.; Powers, R. E.; König, S.; Parac, T. N.; Leary, J. A.; Raymond, K. N. *J. Am. Chem. Soc.* **2001**, *123*, 8923–8938. (l) Sun, X.; Johnson, D. W.; Caulder, D. L.; Powers, R. E.; Raymond, K. N.; Wong, E. H. *J. Am. Chem. Soc.* **2001**, *123*, 2752–2763. (m) Albrecht, M.; Kamptmann, S.; Fröhlich, R. *Polyhedron* **2003**, *22*, 643–647. (n) Albrecht, M.; Janser, I.; Kamptmann, S.; Weis, P.; Wibbeling, B.; Fröhlich, R. *Dalton Trans.* **2004**, 37–43. (o) Albrecht, M.; Janser, I.; Runsink, J.; Raabe, G.; Weis, P.; Fröhlich, R. *Angew. Chem., Int. Ed.* **2004**, *43*, 6662–6666. (p) Albrecht, M.; Janser, I.; Fleischauer, J.; Wang, Y.; Raabe, G.; Fröhlich, R. *Mendeleev Commun.* **2004**, 250–253. (q) Albrecht, M.; Janser, I.; Houjou, H. *Chem.—Eur. J.* **2004**, *10*, 2839–2850. (r) Albrecht, M.; Janser, I.; Hapke, M.; Fröhlich, R.; Weis, P. *Chem.—Eur. J.* **2005**, *11*, 5742–5748. (s) Albrecht, M.; Mirtschin, S.; de Groot, M.; Janser, I.; Runsink, J.; Raabe, G.; Kogej, M.; Schalley, C. A.; Fröhlich, R. *J. Am. Chem. Soc.* **2005**, *127*, 10371–10387. (t) Davis, A. V.; Firman, T. K.; Hay, B. P.; Raymond, K. N. *J. Am. Chem. Soc.* **2006**, *128*, 9484–9496.

(26) Fay, R. C.; Serpone, N. *J. Am. Chem. Soc.* **1968**, *90*, 5701–5706.

Table 4. Optical and Electrochemical Properties of Fc_2Bob Compounds

compound	λ_{max} (Fc absorption)	$E°$, Fe(III,III)/Fe(II,II) V vs Cp_2Fe^+/Cp_2Fe[a]	$E°$, Ti(IV)/Ti(III) V vs Cp_2Fe^+/Cp_2Fe[a]
Fc_2BobH_2	477 nm (2.60 eV)	+0.23	n/a
$(Fc_2Bob)Ti(O^iPr)_2$	489 nm (2.54 eV)	+0.20	< -2.0
$(Fc_2Bob)Ti(OC_6H_4\text{-}2\text{-}OH)_2$	534 nm (2.32 eV)	+0.19	< -2.0
$(Fc_2Bob)Ti(O^iPr)(O_2P[OAr]_2)$[b,c]	540 nm (2.30 eV)	+0.25	< -1.7
$(Fc_2Bob)TiCl_2$	638 nm (1.94 eV)	+0.32	−1.01
$(Fc_2Bob)Ti(O_2P[OAr]_2)_2$[b,d]	653 nm (1.90 eV)	+0.30	−0.83

[a] CH_2Cl_2, 0.1 M $(Bu_4N)PF_6$. [b] Ar = 4-nitrophenyl. [c] The nitrophenyl groups undergo partially reversible reduction at ~ −1.80 V vs Fc. [d] The nitrophenyl groups undergo partially reversible reduction at ~ −1.75 V vs Fc.

are ineffective as π donors. The out-of-plane lone pairs are of pure p-orbital character, but because of interactions with the benzene orbitals, the two combinations are strongly split in energy, rendering only one of them (the higher-energy B_1-symmetry combination) an effective π donor,[27] but this cannot overlap with the unmatched Ti A-symmetry dπ orbital. The monodentate 2-hydroxyphenoxide incurs neither of these limitations (e.g., Ti−O−C = 131.42(15)°, 165.64(14)°) and thus effectively has at least one additional π interaction that is not possible with a chelated catecholate. In a more electron-rich anionic species such as $[Ti(cat)_3]^{2-}$, this additional interaction is evidently too weak to outweigh the entropic advantage of chelation, but it appears to be decisive in the more electron-poor (and π-starved) $(Fc_2Bob)Ti(OC_6H_4\text{-}2\text{-}OH)_2$. Note that $(acac)_2Ti(cat)$ has been prepared, but only by reaction of $\{(cat)Ti(O^iPr)_2\}_n$ with acacH, where no free catechol is present.[28]

Preparation and Characterization of $\{(Fc_2Bob)Ti(\mu\text{-}O)\}_3$. All of the diketonate complexes are water-sensitive to some extent. For example, the diisopropoxide complex $(Fc_2Bob)Ti(O^iPr)_2$ reacts with water in THF over the course of several hours to lose isopropanol and form a cyclic oxo-bridged oligomer. Remarkably, NMR spectra of the crude hydrolysate reveal the presence of only a single oligomer size, and only a single diastereomer of the product, which is revealed by X-ray crystallography to be the D_3-symmetric $(\Delta,\Delta,\Delta)/(\Lambda,\Lambda,\Lambda)$ isomer of the μ-oxo trimer $\{(Fc_2Bob)Ti(\mu\text{-}O)\}_3$ (Figure 2). Dimeric,[29] trimeric,[30] and tetrameric[31] cyclic oxotitanium-bis(diketonate) oligomers have all been characterized structurally, and there is little indication that there is typically much selectivity in their formation (for example, both dimeric[29c] and tetrameric[31] forms of $(^tBuCOCHCO^tBu)_2TiO$ have been reported). As in the catecholate complex, all six ferrocene groups in $\{(Fc_2Bob)Ti(\mu\text{-}O)\}_3$ are again proximal to the biphenyl backbones (Supporting Information, Figure S1), suggesting that this is a general preference for the Fc_2Bob ligand. The Ti−O distances (Table 3, 1.814(6) Å avg.) are similar to those found in $\{(PhCOCHCOPh)_2Ti(\mu\text{-}O)\}_3$ (1.811(6) Å avg.)[30] or in analogous $\{(C_5R_5)Ti(X)(\mu\text{-}O)\}_3$ compounds[32] (1.822(10) Å avg.). The Ti−O−Ti angles (140.1(4)°) are similar to those observed in the dibenzoylmethane trimer (~142°) and somewhat larger than those observed in the cyclopentadienyl trimers (133.9(17)° avg).[33]

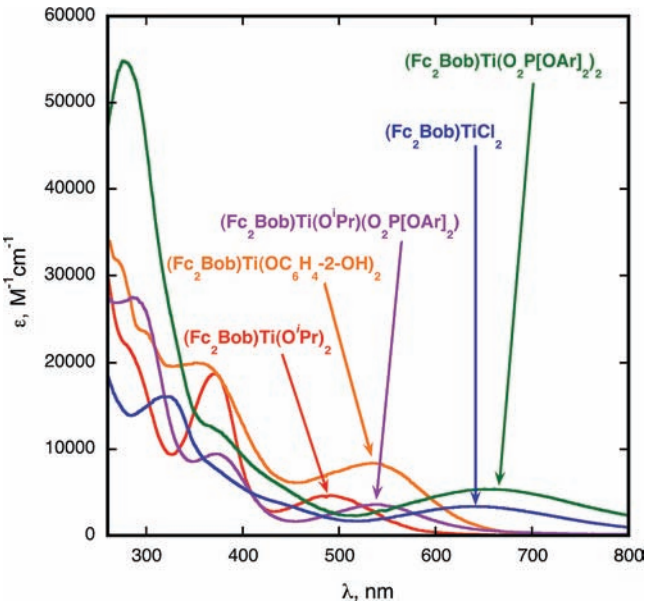

Figure 3. UV−visible spectra of $(Fc_2Bob)Ti(X)(Y)$ complexes (in CH_2Cl_2; Ar = 4-nitrophenyl).

Optical and Electrochemical Properties of Bis(ferrocenyldiketonate)titanium(IV) Complexes. The ferrocenyldiketonate compounds exhibit characteristic, moderately intense ($\varepsilon \sim 10^3$ M^{-1} cm^{-1}) bands in the visible region. These bands are due to the ferrocene units, as they are present even in the free ligand Fc_2BobH_2. While such bands are assigned to d-d transitions in the parent ferrocene,[34] they are known to increase substantially

(27) Gordon, D. J.; Fenske, R. F. *Inorg. Chem.* **1982**, *21*, 2907–2915.
(28) Dahl, G. P.; Block, B. P. *Inorg. Chem.* **1966**, *5*, 1394–1396.
(29) (a) Smith, G. D.; Caughlan, C. N.; Campbell, J. A. *Inorg. Chem.* **1972**, *11*, 2989–2993. (b) Pathak, M.; Bohra, R.; Mehrotra, R. C.; Lorenz, I.-P.; Piotrowski, H. *Trans. Met. Chem.* **2003**, *28*, 187–192. (c) Morozova, N. B.; Turgambaeva, A. E.; Baidina, I. A.; Krysyuk, V. V.; Igumenov, I. K. *J. Struct. Chem.* **2005**, *46*, 1047–1051.
(30) Shi, D.; Dou, G.; Liu, H.; Wang, H. *J. Coord. Chem.* **2008**, *61*, 450–454.
(31) Troyanov, S. I.; Gorbenko, O. Y. *Polyhedron* **1997**, *16*, 777–780.
(32) (a) Blanco, S. G.; Sal, M. P. G.; Carreras, S. M.; Mena, M.; Royo, P.; Serrano, R. *J. Chem. Soc., Chem. Commun.* **1986**, 1572–1573. (b) Troyanov, S. I.; Varga, V.; Mach, K. *J. Organomet. Chem.* **1991**, *402*, 201–207. (c) Carofiglio, T.; Floriani, C.; Sgamellotti, A.; Rosi, M.; Chiesi-Villa, A.; Rizzoli, C. *J. Chem. Soc., Dalton Trans.* **1992**, 1081–1087. (d) Andrés, R.; Galakhov, M.; Gómez-Sal, M. P.; Martín, A.; Mena, M.; Santamaría, C. *J. Organomet. Chem.* **1996**, *526*, 135–143. (e) Amor, J. I.; Cuenca, T.; Galakhov, M.; Gómez-Sal, P.; Manzanero, A.; Royo, P. *J. Organomet. Chem.* **1997**, *535*, 155–168. (f) Kissounko, D. A.; Guzei, I. A.; Gellman, S. H.; Stahl, S. S. *Organometallics* **2005**, *24*, 5208–5210.
(33) An unsymmetrical trimer containing both Cp^*_2Ti and four-coordinate bis(siloxide)titanium fragments has been reported, and shows an unusually wide range of both Ti-(μ-O) bonds (1.730−1.953 Å) and O−Ti−O angles (130.9−140.5°): Edelmann, F. T.; Giessmann, S.; Fischer, A. *J. Organomet. Chem.* **2001**, *620*, 80–89.
(34) Sohn, Y. S.; Hendrickson, D. N.; Gray, H. B. *J. Am. Chem. Soc.* **1971**, *93*, 3603–3612.

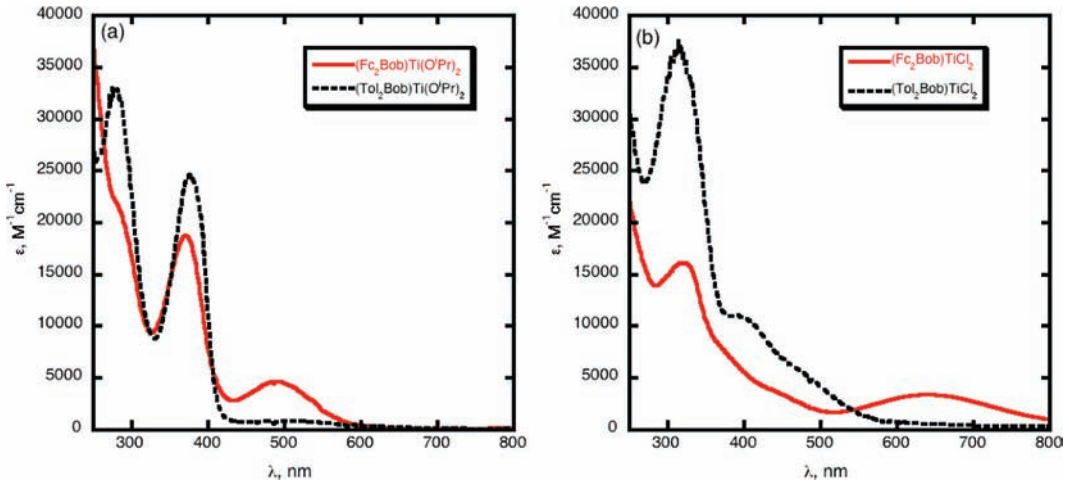

Figure 4. UV−visible spectra of $(Fc_2Bob)TiX_2$ (solid lines) and $(Tol_2Bob)TiX_2$ (dashed lines) in CH_2Cl_2. (a) X = O^iPr; (b) X = Cl.

in intensity in carbonyl-substituted compounds such as acetyl-[35] or benzoylferrocene[36] because conjugation with the carbonyl mixes metal-to-ligand charge-transfer (MLCT) character into the excited state. DFT calculations on the enolized ferrocenyl diketone FcC(OH)=$CHCOCH_3$ support the relevance of this in the diketonates, indicating that while the highest occupied molecular orbital (HOMO) is localized on iron, the lowest unoccupied molecular orbital (LUMO) includes significant contributions from both the iron and the enone π^* system (Supporting Information, Figure S2).

As the ancillary ligands on titanium are varied, the ferrocene-based band in the visible shifts substantially (Table 4), ranging from a λ_{max} of 489 nm for $(Fc_2Bob)Ti(O^iPr)_2$ to 653 nm for $(Fc_2Bob)Ti(O_2P[OC_6H_4NO_2]_2)_2$ (Figure 3). There is a clear trend that the less electron-donating the monodentate anionic ligands on titanium, the more the visible band shifts to lower energy. A similar bathochromic shift also takes place in the more intense, higher-energy bands in the 300−450 nm range. The near-UV bands are clearly due to the $(dike)_2Ti$ core, as they appear in $(Tol_2Bob)TiX_2$ complexes, and indeed the ferrocene groups appear not to perturb these bands significantly, as the appearance of the optical spectra between 300 and 450 nm is virtually the same in, for example, $(Tol_2Bob)Ti(O^iPr)_2$ and $(Tol_2Bob)TiCl_2$ as it is in $(Fc_2Bob)Ti(O^iPr)_2$ and $(Fc_2Bob)TiCl_2$, respectively (Figure 4).

The effect of the ancillary ligands can also be seen in the electrochemistry of the complexes (Table 4). Cyclic voltammetry shows chemically reversible oxidation of the ferrocene groups at potentials slightly more oxidizing than that of Cp_2Fe^+/Cp_2Fe, as expected from the electron-withdrawing effect of the β-diketone group (compare, for example, acetylferrocene, E° = +0.27 V in CH_2Cl_2[12]). The redox waves for the two ferrocene groups are often slightly broadened compared to, say, ferrocene, possibly because of a small amount of splitting, but in no case are they discernibly separated (ΔE° < 60 mV). Most of the compounds do not show any reduction

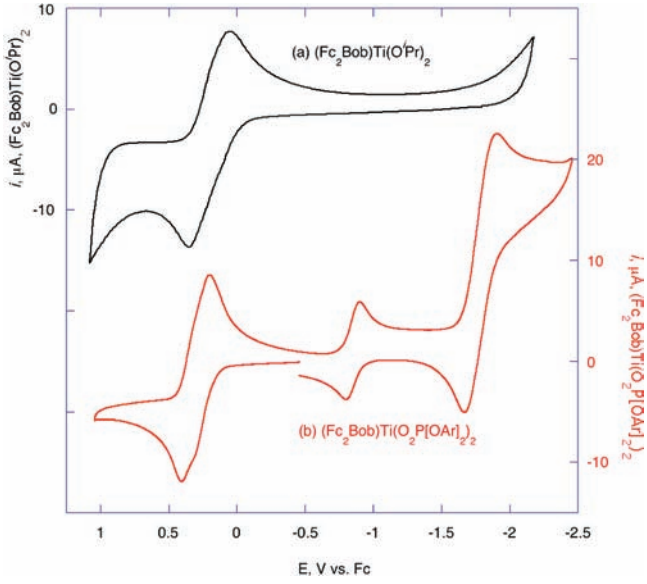

Figure 5. Cyclic voltammograms of (a) $(Fc_2Bob)Ti(O^iPr)_2$ and (b) $(Fc_2Bob)Ti(O_2P[OC_6H_4NO_2]_2)_2$ (CH_2Cl_2, 1 mM complex, 0.1 M $(Bu_4N)PF_6$ supporting electrolyte, scan rate = 60 mV/s). Potentials are given in V vs Cp_2Fe^+/Cp_2Fe.

for the Ti(IV) center at accessible potentials (e.g., Figure 5a, E° < −2.0 V vs Fc), but the most electron-poor compounds, the dichloride and the bis(phosphate), do show a chemically reversible one-electron reduction for the titanium center at ∼ −1.0 V versus Fc (e.g., Figure 5b). The nitrophenylphosphate-containing compounds both show partially reversible multielectron reductions corresponding to reduction of the nitrophenyl groups at ∼ −1.75 V vs Fc, consistent with literature expectations for nitrobenzene radical anion formation (e.g., E° for 4-nitroanisole, −1.25 V vs SCE, −1.7 V vs ferrocene/ferrocenium).[37]

The variation of both the optical and the electrochemical properties with the nature of the ancillary ligands on titanium can be understood on the basis of the electronic structure of the complexes. The HOMOs of the complexes, as on the free ligand, are largely

(35) Tarr, A. M.; Wiles, D. M. *Can. J. Chem.* **1968**, *46*, 2725–2731.
(36) Yamaguchi, Y.; Ding, W.; Sanderson, C. T.; Borden, M. L.; Morgan, M. J.; Kutal, C. *Coord. Chem. Rev.* **2007**, *251*, 515–524.
(37) Maki, A. H.; Geske, D. H. *J. Am. Chem. Soc.* **1961**, *83*, 1852–1860.

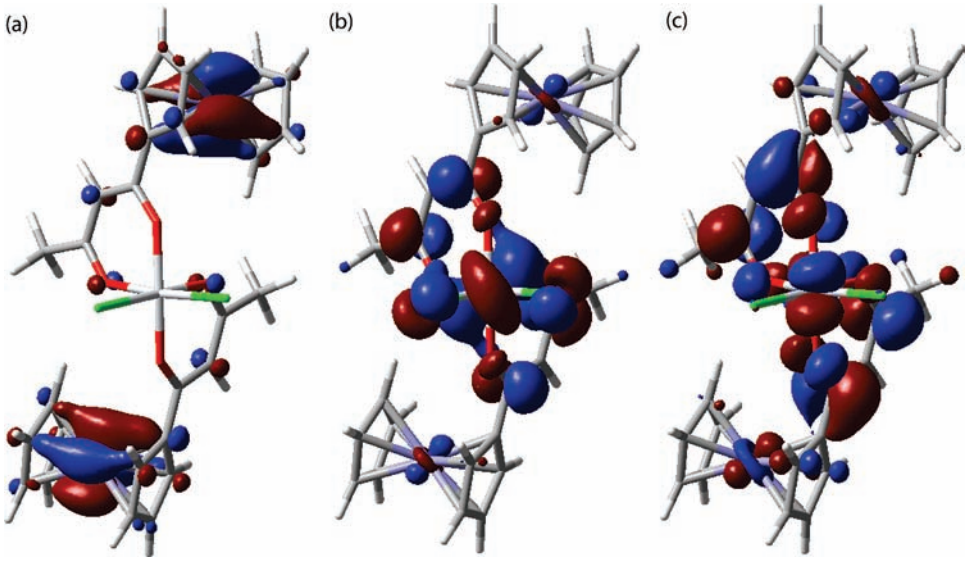

Figure 6. Calculated Kohn−Sham orbitals of $(FcCOCHCOCH_3)_2TiCl_2$ (B3LYP, 6-31G*). (a) HOMO, $E = -5.610$ eV. (b) LUMO, $E = -2.817$ eV. (c) LUMO + 3, $E = -1.523$ eV.

iron-localized orbitals that interact very little with the titanium center (Figure 6a). For example, while the potential of the titanium(IV)/(III) redox couple shifts dramatically on changing from $(Fc_2Bob)Ti(O^iPr)_2$ to $(Fc_2Bob)Ti(O_2P[OC_6H_4NO_2]_2)_2$ (>1.2 V), the Fe(II)/Fe(III) potential shifts less than 100 mV. Because the titanium interacts little with the filled iron-based orbitals from which electrons are removed on oxidation, the HOMO and HOMO-1 are barely split in the complex (the calculated splitting is 0.004 eV in $(FcCOCHCOCH_3)_2TiCl_2$). The two ferrocene units act essentially independently on oxidation, and the two Fe(II)/(III) couples occur at essentially the same potential.

While the high-lying filled orbitals are not sensitive to the electronic structure of the titanium, the low-lying empty orbitals are (Figures 6b,c). An earlier analysis of the electronic structure of $(acac)_2TiCl_2$ noted the greater interaction of the titanium dπ orbitals with the LUMOs of the acac ligands than with their HOMOs, presumably because of the better energy match between the former orbitals and the orbitals on the electropositive titanium.[9] The same effect is apparent here, with a set of orbitals that are principally titanium dπ in character, with some diketonate π^* character (e.g., Figure 6b), and a higher-lying set of orbitals that are principally diketonate π^*, with some titanium dπ character mixed in (Figure 6c).

Given the substantial contributions of the titanium dπ orbitals to the low-lying virtual orbitals, it is reasonable to expect that visible ferrocene-to-ligand π^* will acquire substantial charge-transfer character in the metal complexes. This analysis is supported by time-dependent DFT (TD-DFT) calculations on $(FcCOCHCOCH_3)_2TiCl_2$ (see Supporting Information), which show that the lowest-energy excitations involve substantial participation by both the largely titanium-centered orbitals (the LUMO and LUMO+1, e.g., Figure 6b) and the largely diketonate π^* orbitals (the LUMO+3 and LUMO+4, e.g., Figure 6c). The involvement of the ligand π^* orbitals in the visible bands is critical: if they were due to a simple Fc-to-Ti charge transfer, one would expect an additional band to appear on complexation of the ligand to titanium, but instead only a shift of the band is observed. Likewise, the highest-lying titanium dπ orbital (LUMO+2), which does not mix with the diketonate π^* orbitals,[9] is not involved significantly in the low-lying excitations according to the TD-DFT calculations. This analysis is qualitatively consistent with the published analysis of the near-UV bands of $(dike)_2TiX_2$ complexes, which were assigned to ligand $\pi-\pi^*$ transitions, with modest mixing of ligand-to-metal charge transfer character into the excited state.[38] The substantial mixing of the titanium dπ levels with the ligand π^* levels provides an efficient route for communication of the electronic changes at titanium to the ferrocene-based electronic transitions, even in the absence of direct interactions between the filled iron-based orbitals with the titanium center.

Conclusions

The 2,2′-biphenylbis(2,4-dioxobutane) (Bob) framework allows the preparation of a series of ferrocenyldiketonate titanium(IV) complexes of predictable structure. The interaction of the π system of the diketonates with the titanium center has a profound impact on the reactivity and the optical and electrochemical properties of these compounds. For example, reaction of $(Fc_2Bob)Ti(O^iPr)_2$ with catechol gives the bis(2-hydroxyphenoxide) complex $(Fc_2Bob)Ti(O-C_6H_4-2-OH)_2$ rather than the chelated catecholate complex, presumably because the relatively weak π donation of the diketonate ligands to titanium favors κ^1 binding and stronger π donation from the catechol. Interaction of the π^* orbitals of the diketonate with the titanium dπ orbitals is particularly strong, resulting in dramatic shifts of the color of the complexes (due to ferrocenyl-to-diketonate π^* transitions) as a function of the ancillary ligands X in $(Fc_2Bob)TiX_2$. No strong intermetallic communication is evident in the electrochemistry of the complexes, where only modest shifts in potential and undetectably small splitting of the ferrocene

(38) Schmidtke, H.-H.; Voets, U. *Inorg. Chem.* **1981**, *20*, 2766–2771.

redox waves are observed, since the electrochemistry is governed not by the π^* orbitals but by the high-lying filled orbitals that are largely localized on iron and interact very weakly with titanium.

Acknowledgment. This work was supported by the National Science Foundation (CHE-0518243). L.T.D. and E.O. thank the Notre Dame Nano-Bio REU program (NSF EEC-0354134) for summer support. Partial support for the X-ray diffraction facility was provided by the NSF (CHE-0443233).

Supporting Information Available: Crystallographic information on $(Fc_2Bob)Ti(OC_6H_4\text{-}2\text{-}OH)_2$ and $\{(Fc_2Bob)Ti(\mu\text{-}O)\}_3 \cdot 2CHCl_3 \cdot 2THF$ in CIF format; alternative views of the conformations of $(Fc_2Bob)TiX_2$ and details of calculations on $FcC(OH)=CHCOCH_3$ and $(FcCOCHCOCH_3)_2TiCl_2$ (PDF format). This material is available free of charge via the Internet at http://pubs.acs.org.